Supplementary Information

Regulating the Size and Assembled Structure of Graphene Building Blocks for High-Performance Silicon Nanocomposite Anodes

Bo Nie,[a] David Sanchez,[b] Mataz Alcoutlabi,[b] Tengxiao Liu,[c] Saurabh Basu,[a] Soundar Kumara,[a] Gongkai Wang[d*] and Hongtao Sun,[a,e*]

[a]*The Harold & Inge Marcus Department of Industrial & Manufacturing Engineering, The Pennsylvania State University, University Park 16802, Pennsylvania, USA.*

[b]*Department of Mechanical Engineering, The University of Texas, Rio Grande Valley 78539, Texas, USA*

[c]*Department of Biomedical Engineering, The Pennsylvania State University, University Park 16802, Pennsylvania, USA.*

[d]*Tianjin Key Laboratory of Materials Laminating Fabrication and Interface Control Technology, School of Material Science and Engineering, Hebei University of Technology, Tianjin, 300130, China.*

[e]*Materials Research Institute (MRI), The Pennsylvania State University, University Park 16802, Pennsylvania, USA.*

*Corresponding author.
Email address: hongtao.sun@psu.edu (H. Sun); tql5160@psu.edu (T. Liu);
wang.gongkai@hebut.edu.cn (G. Wang);

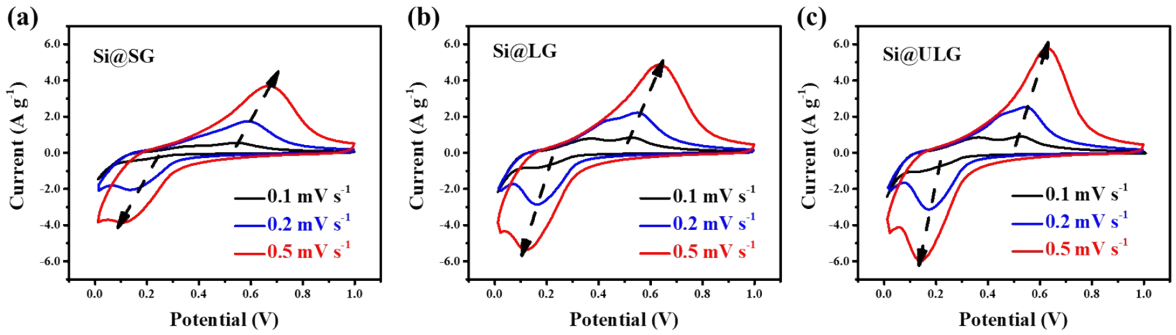

Fig. S1. The cyclic voltammetry curves for the Si@ULG, Si@LG, and Si@SG nanocomposite anodes at scan rates of 0.1, 0.2, and 0.5 mV s^{-1}.

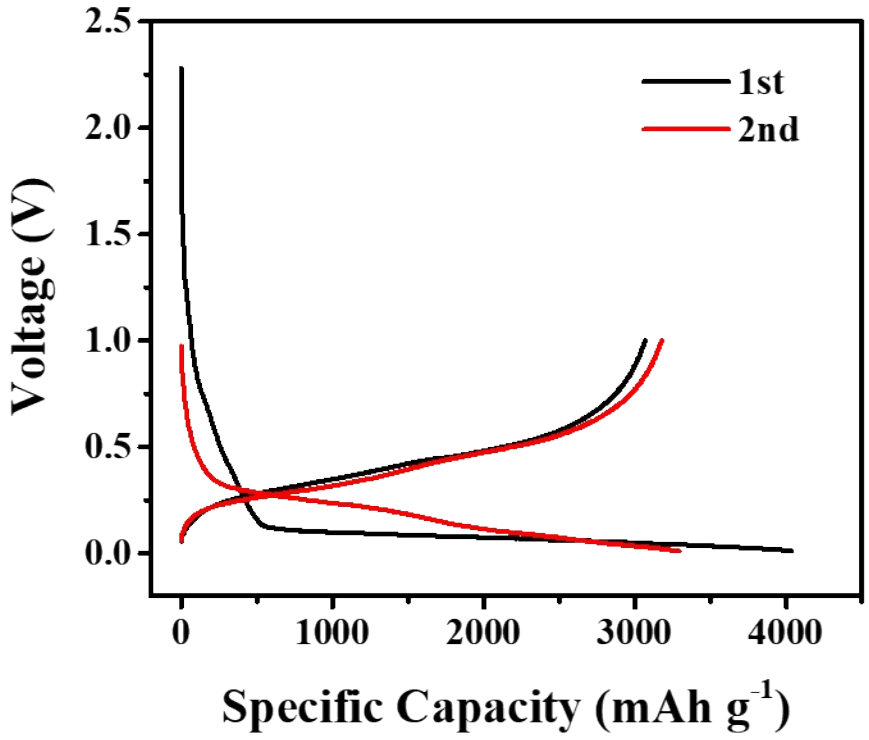

Fig. S2. The first two charge-discharge curves for the Si@ULG nanocomposite anode at C/20.

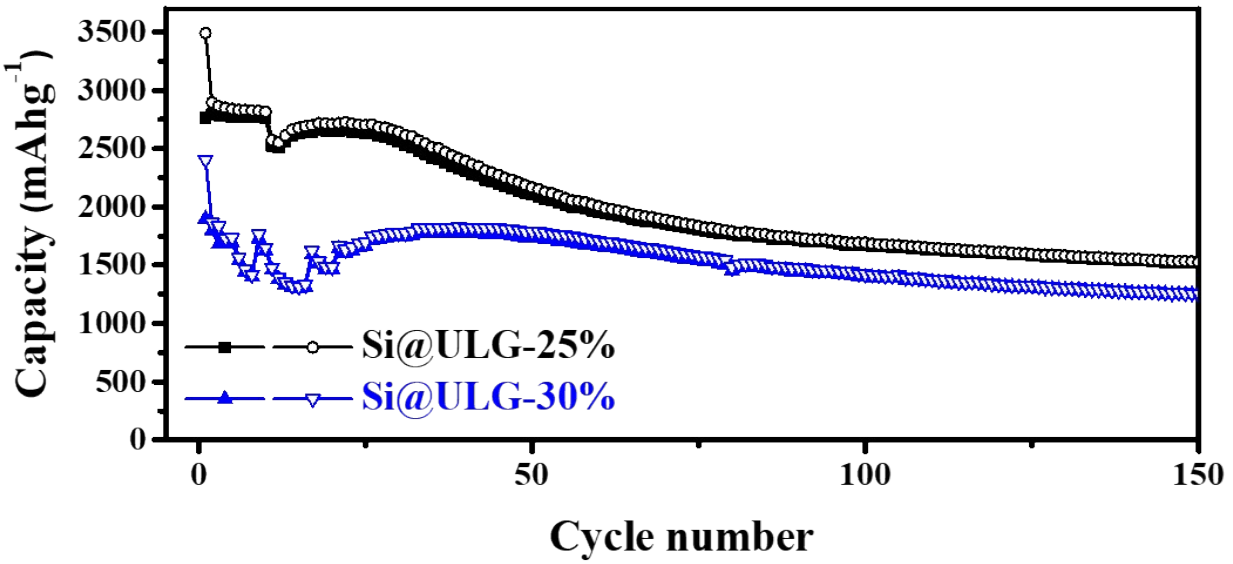

Fig. S3. The cyclic performance of Si@ULG nanocomposite electrode with different ULG weight percentages at C/5.

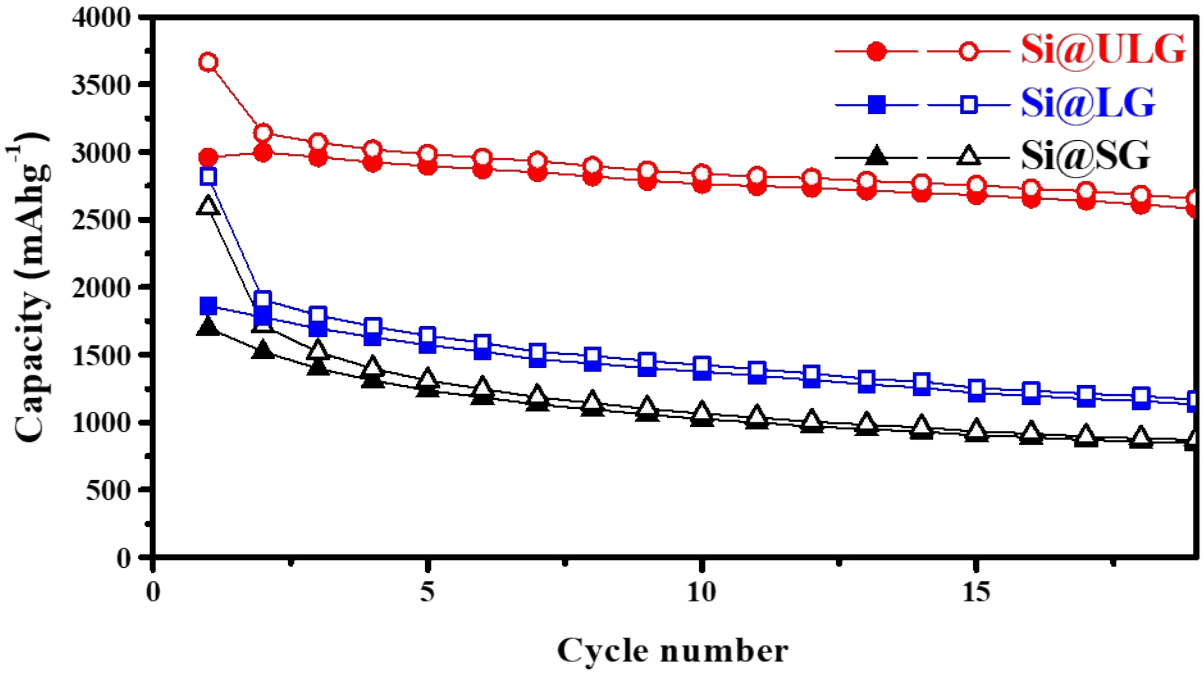

Fig. S4. The cyclic performance of the Si@ULG, SI@LG, and Si@SG nanocomposite electrodes using PVDF binders at C/20.

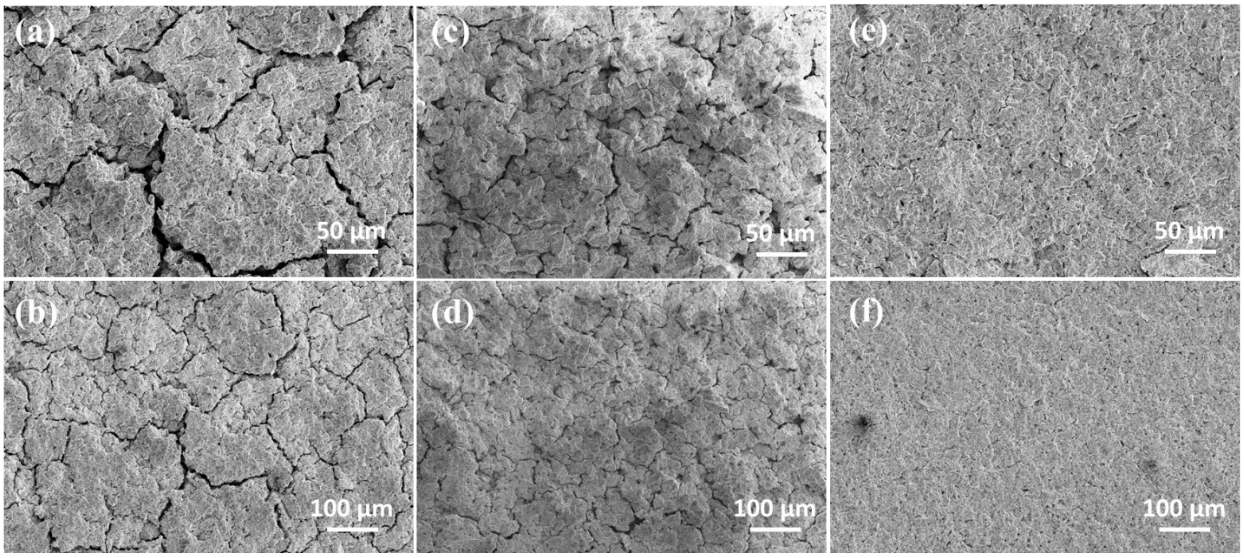

Fig. S5 The SEM images of the Si-graphene composite electrodes after 50 cycles at 0.2 C. **(a, b),** Si@SG; **(c, d),** Si@LG; and **(e, f),** Si@ULG.

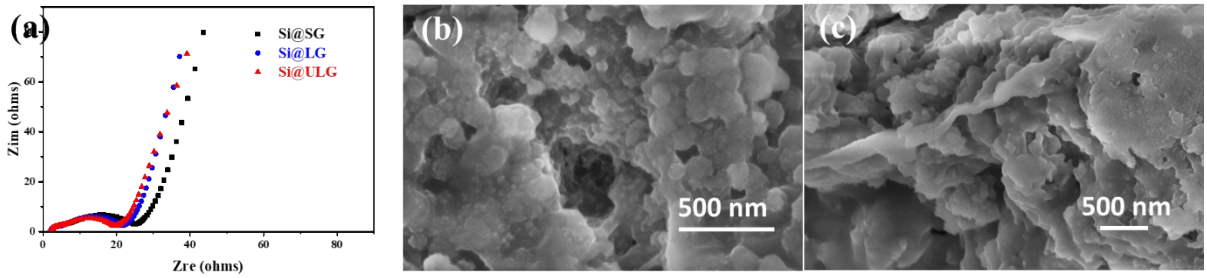

Fig. S6. **(a)** The EIS of the Si-graphene electrodes after 50 cycles at 0.2C; **(b, c)** the higher magnification images of the cycled Si@ULG electrode.

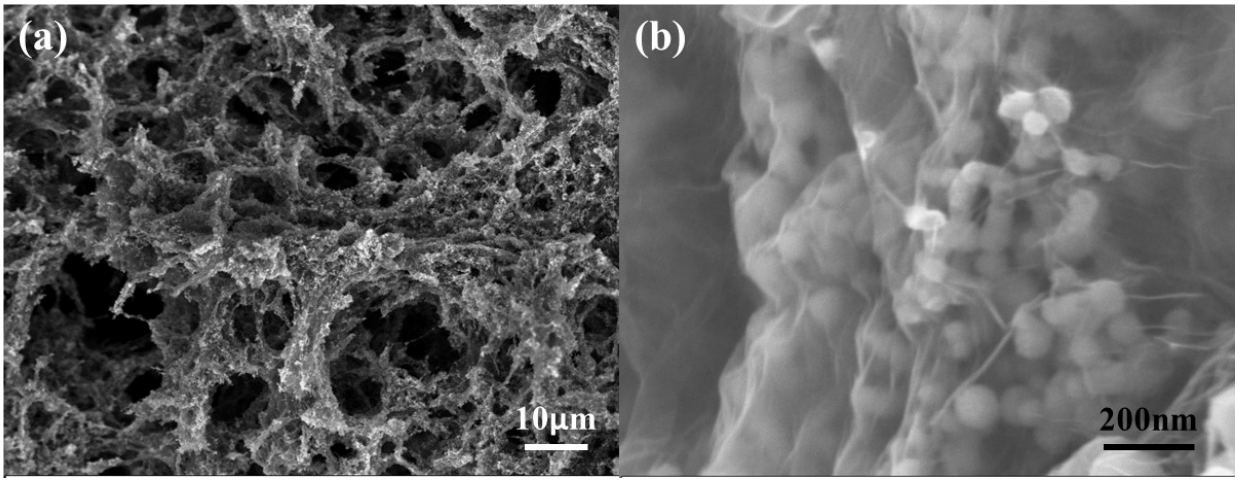

Fig. S7. Morphology characterization via SEM of freestanding 3D Si@ULG-ULG nanocomposite electrode at low magnification (**a)**, and high magnification (**b)**.

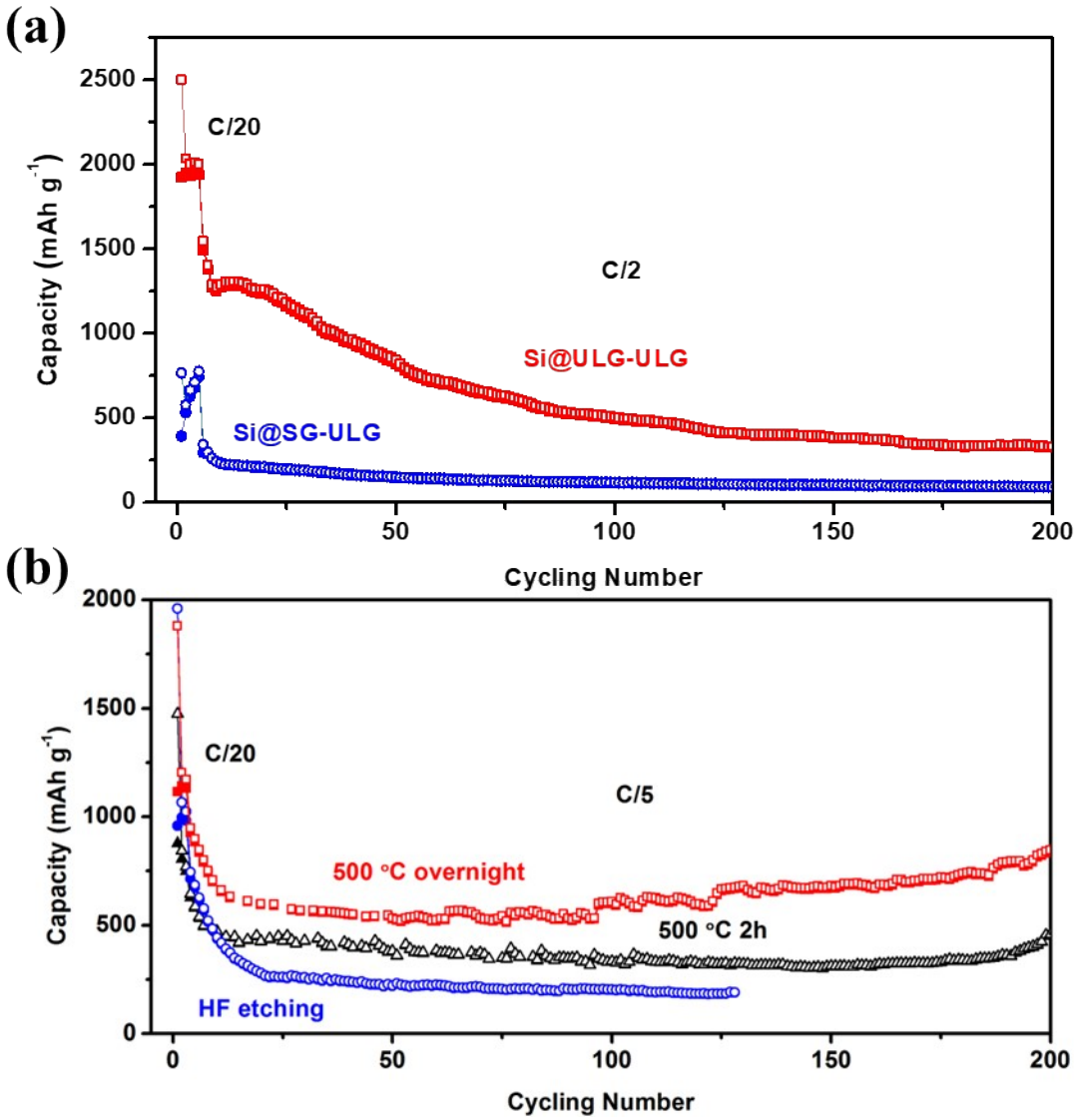

Fig. S8. (a) The cyclic performance of various 3D freestanding nanocomposite anodes with different sizes of graphene sheets at C/2. **(b)** The influence of affinity on the electrochemical performance by tuning the oxidation layer on the surface of Si and remaining function groups in reduced GO sheets (Si@ULG-ULG).

Table S1. The fitted results from the Nyquist plot of the Si@ULG composite half cells.

Sample	R_0 (ohm)	R_{ct} (ohm)	W (ohm)
Si@ULG	1.92	74.8	1.4
Si@LG	1.47	137.5	122
Si@SG	0.27	290.4	269.2

Table S2. The capacity retention of the Si@ULG nanocomposite electrodes with different percentages of ULG.

Sample	1^{st} Charge Capacity (0.2 C)	150^{th} Charge Capacity (0.2 C)	Retention
Si@ULG 30%	1603	1260	79%
Si@ULG 25%	2524	1540	60%

Table S3. The comparison of Si@graphene composite with the reported Si composite electrodes.

Electrodes	Areal Mass Loading (mg cm^{-2})	Gravimetric Capacity) (mAh g^{-1})	Capacity loss per cycle (cycles)	Current Density (mA g^{-1})	Reference
Si@ULG composite	0.26	2751	0.23% (200)	840	**This work**
3D Si@ULG-ULG	3	1800	0.2% (250)	840	
Si/graphene composite	NA	2158	1.5%	100	[1]
Si@graphene cage composite	NA	~2100	0.28% (200)	1000	[2]
rGO-porous Si composite	0.33	~1750	0.26% (200)	1000	[3]
SiNP@graphene cage/GNS	NA	2449	0.2% (200)	1000	[4]
rGO/Si composites	1.35	2500	0.25% (300)	210	[5]
3D Si@rGO composite	2.6	2963	0.27% (200)	500	[6]
Sputtered Si on CVD-rMGO	0.23	~1200	0.33% (90)	132	[7]

Reference:

[1] Chou, S.L., Wang, J.Z., Choucair, M., Liu, H.K., Stride, J.A. and Dou, S.X., Enhanced reversible lithium storage in a nanosize silicon/graphene composite. Electrochem. Commun. 2010, 12(2), pp.303-306.

[2] Nie, P., Le, Z. Y., Chen, G., Liu, D., Liu, X. Y., Wu, H. B., Xu, P. C., Li, X. R., Liu, F., Chang, L. M., Zhang, X. G., Lu, Y. F., Graphene Caging Silicon Particles for High-Performance Lithium-Ion Batteries, Small 2018, 14, 1800635.

[3] Jiao, L.S., Liu, J.Y., Li, H.Y., Wu, T.S., Li, F., Wang, H.Y. and Niu, L., Facile synthesis of reduced graphene oxide-porous silicon composite as superior anode material for lithium-ion battery anodes. J. Power Sources, 2016, 315, pp.9-15.

[4] Han, X.Y., Zhao, D.L., Meng, W.J., Yang, H.X., Zhao, M., Duan, Y.J. and Tian, X.M., Graphene caging silicon nanoparticles anchored on graphene sheets for high performance Li-ion batteries. Applied Surface Science, 2019, 484, pp.11-20.

[5] Yue, H., Li, Q., Liu, D., Hou, X., Bai, S., Lin, S. and He, D., High-yield fabrication of graphene-wrapped silicon nanoparticles for self-support and binder-free anodes of lithium-ion batteries. J. Alloys Compd., 2018, 744, pp.243-251.

[6] Wasalathilake, K.C., Hapuarachchi, S.N., Zhao, Y., Fernando, J.F., Chen, H., Nerkar, J.Y., Golberg, D., Zhang, S. and Yan, C., Unveiling the working mechanism of graphene bubble film/silicon composite anodes in Li-ion batteries: from experiment to modeling. ACS Appl. Energy Mater., 2019, 3(1), pp.521-531.

[7] Lockett, M., Sarmiento, V., Gonzalez, M., Ahn, S., Wang, J., Liu, P. and Vazquez-Mena, O., Ultrathin 5 μm Thick Silicon Nanowires Intercalated with Reduced Graphene Oxide Binderless Anode for Lithium-Ion Batteries. ACS Appl. Energy Mater., 2021, 4(7), pp.6391-6398.